• Basic Research •

Identification of hub genes for glaucoma: a study based on bioinformatics analysis and experimental verification

Rui-Ling Xie[1], *Hai-Yan Nie*[1], *Yu-Xin Xu*[2]

[1]Department of Ophthalmology, Anhui Public Health Clinical Center, the First Affiliated Hospital of Anhui University North District, Hefei 230000, Anhui Province, China
[2]Department of Ophthalmology, the Second Hospital of Anhui Medical University, Hefei 230000, Anhui Province, China
Correspondence to: Rui-Ling Xie and Yu-Xin Xu. No.100, Huaihai Avenue, Hefei 230000, Anhui Province, China. xieruilinghf@163.com; xuyuxin1168@sina.com
Received: 2023-03-16 Accepted: 2023-05-24

Abstract

● **AIM:** To explore hub genes for glaucoma based on bioinformatics analysis and an experimental model verification.

● **METHODS:** In the Gene Expression Omnibus (GEO) database, the GSE25812 and GSE26299 datasets were selected to analyze differentially expressed genes (DEGs) by the GEO2R tool. Through bioinformatics analysis, 9 hub genes were identified. Receiver operating characteristic (ROC) curves and principal component analysis (PCA) were performed to verify whether the hub gene can distinguish glaucoma from normal eyes. The mouse model of glaucoma was constructed, and the real-time reverse transcriptase-polymerase chain reaction (RT-qPCR) assay was performed to detect the expression levels of hub genes in glaucoma.

● **RESULTS:** There were 128 overlapping DEGs in the GSE25812 and GSE26299 datasets, mainly involved in intracellular signalling, cell adhesion molecules and the Ras signalling pathway. A total of 9 hub genes were screened out, including GNAL, BGN, ETS2, FCGP4, MAPK10, MMP15, STAT1, TSPAN8, and VCAM1. The area under the curve (AUC) values of 9 hub genes were greater than 0.8. The PC1 axle could provide a 70.5% interpretation rate to distinguish glaucoma from normal eyes. In the ocular tissues of glaucoma in the mice model, the expression of BGN, ETS2, FCGR4, STAT1, TSPAN8, and VCAM1 was increased, while the expression of GNAL, MAPK10, and MMP15 was decreased.

● **CONCLUSION:** Nine hub genes in glaucoma are identified, which may provide new biomarkers and therapeutic targets for glaucoma.

● **KEYWORDS:** glaucoma; biomarkers; hub genes

DOI:10.18240/ijo.2023.07.03

Citation: Xie RL, Nie HY, Xu YX. Identification of hub genes for glaucoma: a study based on bioinformatics analysis and experimental verification. *Int J Ophthalmol* 2023;16(7):1015-1025

INTRODUCTION

Glaucoma, the second leading cause of blindness, is a group of chronic progressive optic nerve diseases[1]. It is estimated that 111.8 million people will have glaucoma due to the expansion of the ageing population in 2040[2]. Currently, lasers therapy, and drugs are the main treatments for glaucoma[3-5]. But other diseases are induced in the treatment of glaucoma, such as corneal endothelial cell loss, causing corneal decompensation[6]. Therefore, it is extremely important to further explore the molecular mechanisms and therapeutic targets of glaucoma.

Glaucoma is characterized by loss of retinal ganglion cells, thinning of the retinal nerve fiber layer, and progressive depression of the optic nerve disc[7]. Elevated intraocular pressure (IOP) is the most important predisposing factor for glaucoma[8]. Glaucoma is influenced by genetic factors. Early-onset, which occurs before age 40, is associated with Mendelian inheritance, and adult-onset glaucoma has complex genetic features[9]. Mutations in *OPTN* and *TBK1* account for approximately 2%-3% of familial normal-tension glaucoma, inducing patients to develop the disease before the age of 40y[10-11]. In addition, the vascular endothelial growth factor (VEGF) family is a key inducer of corneal neovascularization, consisting of positive regulators of retinal angiogenesis[12-13]. Studies have shown that VEGF-A gene showed significant changes in expression upon recovery from hypoxic tissue damage in retinal diseases and in proliferative vitreoretinopathy samples[14-15].

In recent years, with the rapid development of bioinformatics and high-throughput sequencing, a growing number of genes related to glaucoma have been identified. The GSE218153 gene expression profile in the Gene Expression Omnibus (GEO) database shows that *TIPARP* is associated with IOP regulation[16]. Margeta *et al*[17] found that Apoe and Galectin-3 are upregulated in the glaucomatous retina and during the transformation of microglia into a neurodegenerative

phenotype, as revealed by high-throughput sequencing. Further study shows that diminished activation of APOE4 microglia offers protection in glaucoma, and targeting APOE-Galectin-3 signaling presents a potential therapeutic strategy for this vision-impairing condition[18]. However, the underlying molecular mechanisms are not fully understood and need to be further explored for better clinical application.

In this study, the GSE25812 and GSE26299 datasets from the GEO dataset were selected to analyze differentially expressed genes (DEGs). Hub genes were identified by bioinformatics analysis. Hub gene expression was experimentally validated by constructing a mouse model of glaucoma. This study may provide new biomarkers and therapeutic targets for glaucoma.

MATERIALS AND METHODS

Ethical Approval All experimental protocols were approved by the Animal Ethics Committee of Anhui Medical University. (No.LLSC20221257). All methods were carried out in accordance with the Guide for the Care and Use of Laboratory Animals. All methods are reported in accordance with ARRIVE guidelines for the reporting of animal experiments. The study was carried out in accordance with the relevant guidelines and regulation.

Microarray Data Source We selected the GSE25812 (GPL6887, Illumina MouseWG-6 v2.0 expression beadchip) and GSE26299 [GPL1261, (Mouse430_2) Affymetrix Mouse Genome 430 2.0 Array] datasets from the GEO database. Three non-glaucomatous samples and three glaucomatous samples in the GSE25812 dataset were selected. Ten non-glaucomatous samples and ten glaucomatous samples in the GSE26299 dataset were chosen for analysis.

Identification of Differentially Expressed Genes The GSE25812 and GSE26299 datasets were analyzed using the GEO2R tool (www.ncbi.nlm.nih.gov/geo/geo2r). The overlapping DEGs of the two datasets were identified by plotting the Venn diagram (http://jvenn.toulouse.inra.fr/app/example.html).

Functional Enrichment Analysis of Differentially Expressed Genes Gene Ontology (GO) functional enrichment analysis and Kyoto Encyclopedia of Genes and Genomes (KEGG) pathway enrichment analysis for the overlapping DEGs were performed in the Database for Annotation, Visualization, and Integrated Discovery database (https://david.ncifcrf.gov/). Box plots and bubble plots for the top 6 GO terms and the top 8 KEGG pathways based on *P*-values were then plotted using the cluster Profiler package in R software (version 3.6.1).

Construction of the Protein-Protein Interactions Network and Identification of Hub Genes The DEGs were analyzed using the STRING (https://www.string-db.org/) online database to predict the interaction relationships between proteins encoded by DEGs. For the significance criteria, the confidence interaction score was set at 0.15. The protein-protein interactions (PPI) network was visualized using Cytoscape software (version 3.9.1). Hub modules were identified using the Molecular Complex Detection (MCODE) plug-in. The screening criteria were: Degree cutoff ≥2, node score cutoff ≥0.2, K-core ≥2, and max depth=100.

Analysis of Hub Genes We mapped the ridge plot of hub genes expression as well as screened for diagnostic biomarkers of glaucoma by receiver operating characteristic (ROC) curves analysis and principal component analysis (PCA). The corresponding area under the ROC curve (AUC) greater than 0.5 was considered to be significant. An interpretation rate of greater than 50% for the PC axis was considered significant.

Construction of a Model Mouse for Glaucoma We induced glaucoma in the eye of mice by injecting magnetic microbeads[19]. C57 mice (6-8 weeks old, weighing 18-20 g, SPF Biotechnology Co. Ltd., Beijing, China) were used to generate the glaucoma models. Two days before the anterior chamber injection, mice were treated with ofloxacin hydrochloride eye drops (H20067760, Shanglinag Pharmaceutical, Jiangxi Province, China) for against infection. The eyes of the mice were dilated with compound tropicamide drops (J20180051, Santen, Pharmaceutical, Osaka, Japan), and then injected with intramuscular injection of Zoletil 50 [8ADTA, Virbac Trading (Shanhai), Shanhai, China] and xylazine hydrochloride injection (20210308, Fangzheng, Pharmaceutical, Jilin, China), at doses of 10 and 4 mg/kg, respectively, for general anesthesia and corneal surface anesthesia. Approximately l-2 mm away from the cornea at the corneoscleral limbus of the mice, an insulin syringe with a needle diameter of 30 G (Yeso-med, Wuxi, China) was injected into the anterior chamber with 20 μL of a suspension of silica magnetic beads (Knowledge & Benefit Sphere, Suzhou, China) at a concentration of 50 mg/mL. The mice were then placed intraoperatively with their eyes up on a warming pad and cared for until awakening. After 14d, mice were anesthetized by intraperitoneal injection of Zoletil 50 and xylazine hydrochloride injection. After cervical dislocation execution, the eyes of the mice were immediately removed and immersed in paraformaldehyde.

Hematoxylin-Eosin Staining Tissue from each group of mouse eye tissue was taken and placed in 4% paraformaldehyde solution for fixation. After dehydration in ethanol, the tissue was embedded in paraffin impregnation and sectioned to 4 microns for hematoxylin-eosin (HE) staining. The mouse eye tissue physiological changes were observed under a light microscope (OLYMPUS, Japan) and photographed.

Real-time Reverse Transcriptase - Quantitative Polymerase Chain Reaction Assay We have referred to the relevant literature for the specific experimental steps of reverse transcriptase - quantitative polymerase chain reaction (RT-qPCR)[20]. The primer sequences used are shown in Table 1.

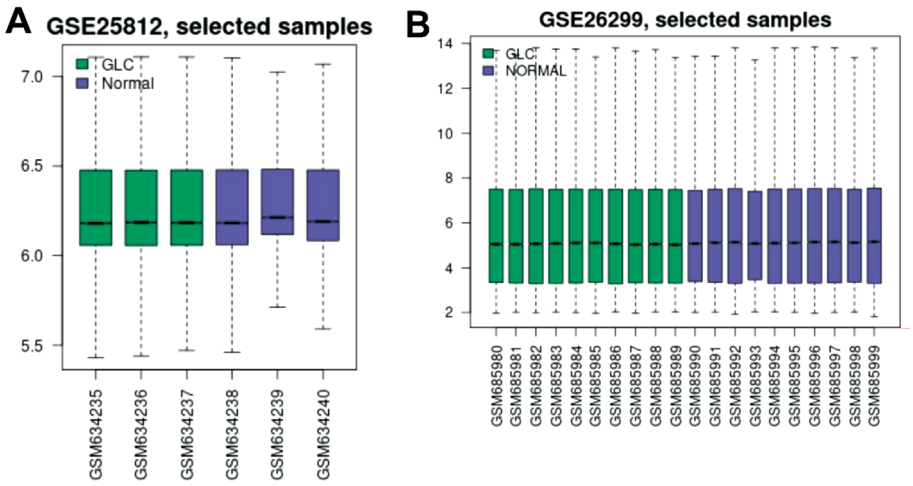

Figure 1 Normalization to samples in the GSE25812 and the GSE26299 datasets A: Cross-comparability evaluation of data set samples in the GSE25812; B: Cross-comparability evaluation of data set samples in the GSE26299 dataset.

Statistical Analysis GraphPad Prism 9 (version 9.5.0.730) was used to conduct the statistical analysis. To compare continuous variables between the two groups, an unpaired *t*-test was conducted. $P<0.05$ was regarded as statistically significant.

RESULTS

Identification of Differentially Expressed Genes GSE25812 and GSE26299 datasets were downloaded from the GEO database to screen DEGs. The GSE25812 dataset contains 6 samples: 3 non-glaucomatous samples (control) and 3 glaucomatous samples (model). Meanwhile, the GSE26299 has 20 samples, including 10 non-glaucomatous samples (control) and 10 glaucomatous samples (model). We first standardized the read counts for each sample in GSE25812 and GSE26299 datasets. The findings revealed that the median values are nearly identical for each sample (Figure 1A: GSE25812, Figure 1B: GSE26299), demonstrating that the GSE25812 and GSE26299 datasets fit the criteria for further research. There were 1737 DEGs in the GSE25812 dataset, of which 742 were up-regulated, and 995 were down-regulated (Figure 2A). In the GSE26299 dataset, there were 1532 DEGs, including 647 up-regulated genes and 885 down-regulated genes (Figure 2B). Then we plotted the heatmap of the top 25 up-regulated and down-regulated genes (Tables 2 and 3) according to *P* value in the GSE25812 and GSE26299 datasets (Figure 2C and 2D). Venn diagram showed that there were 128 overlapping DEGs for GSE25812 and GSE26299 datasets (Figure 3).

Functional Enrichment Analysis of Overlapping Differentially Expressed Genes GO annotation analysis and KEGG pathway analysis was performed in the DAVID database to explore the potential molecular functions of the overlapping DEGs. According to *P*-value, the top 6 GO terms with the most significant enrichment were picked out, and the results were shown in the bubble plot of GO enrichment analysis (Figure 4A). The results showed that in the MF category, the DEGs primarily had an essential correlation with protein kinase binding, protein serine/threonine kinase activity and metal ion binding. For the BP category, the DEGs were mainly involved in neural crest cell migration, vasodilation and TOR signaling. For the CC category, the DEGs were mainly enriched in the cell surface, nucleoplasm and endoplasmic reticulum. According to p-value, the top 8 KEGG pathways with the most significant enrichment were picked out, and the results are shown in the bubble plot of KEGG pathways enrichment analysis (Figure 4B). The results showed that the DEGs were mainly enriched in expression and PD-1 checkpoint pathway in cancer, cell adhesion molecules and Ras signaling pathway.

Table 1 Primer sequence information used in this study

Name	Sequences (5′-3′)
GAPDH-F	CTCATGACCACAGTCCATGC
GAPDH-R	TTCAGCTCTGGGATGACCTT
GNAL-F	GCTGGCAGAAAAAGTCTTGG
GNAL-R	GCAGGTGAAGTGAGGGTAGC
BGN-F	GACAACCGTATCCGCAAAGT
BGN-R	GTGGTCCAGGTGAAGTTCGT
ETS2-F	AATGCAGGCACCAAACTACC
ETS2-R	GTCCTGGCTGATGGAACAGT
FCGR4-F	AACGGCAAAGGCAAGAAGTA
FCGR4-R	CCGCACAGAGAAATACAGCA

Construction of PPI Networks and Identification of Hub Genes A PPI network was constructed in the STRING database to analyze the interactions of the overlapping DEGs. The PPI network consists of 76 genes (Figure 5). Then the PPI network was visualized by Cytoscape software. The MCODE was then used to identify highly interconnected clusters from the PPI network of DEGs as potential functional molecular complexes for glaucoma, from which nine hub genes were

Table 2 The top 25 DEGs of the up-regulated versus down-regulated genes in the GSE25812 dataset

Name	Description	log_2 fold change	*P*	Up/down
Tdrd7	Tudor domain containing 7	3.50	3.90E-11	Up
Snhg12	Small nucleolar RNA host gene 12	1.73	9.83E-08	Up
Ttc27	Tetratricopeptide repeat domain 27	1.13	1.27E-03	Up
Hspb1	Heat shock protein 1	0.99	5.20E-05	Up
ND5	NADH dehydrogenase subunit 5	0.94	1.33E-02	Up
Actb	Heat shock protein 8	0.81	2.84E-03	Up
Fbxo10	Actin, beta	0.78	2.35E-02	Up
Ppm1e	Actin, beta	0.75	4.36E-02	Up
Snx22	F-box protein 10	0.75	1.10E-03	Up
AA467197	RIKEN cDNA 5430416N02 gene	0.63	8.57E-06	Up
Ccdc117	Protein phosphatase 1E (PP2C domain containing)	0.63	3.49E-06	Up
Cryab	Sorting nexin 22	0.63	2.38E-05	Up
Lin7a	Kelch-like 22	0.63	4.67E-04	Up
Ints3	Expressed sequence AA467197	0.62	3.01E-04	Up
H2-Eb1	Coiled-coil domain containing 117	0.61	6.24E-03	Up
Gm11837	Crystallin, alpha B	0.58	6.57E-03	Up
Uba6	Lin-7 homolog A (C. elegans)	0.57	1.12E-02	Up
Tmem254a	Integrator complex subunit 3	0.55	5.38E-05	Up
Gadd45a	Histocompatibility 2, class II antigen E beta	0.54	7.26E-04	Up
Abcc5	Predicted gene 11837	0.52	3.15E-02	Up
Ceacam2	Ubiquitin-like modifier activating enzyme 6	0.51	4.36E-02	Up
Hfe	RIKEN cDNA 1300017J02 gene	0.51	5.01E-05	Up
Ndufa5	Transmembrane protein 254a	0.50	4.21E-02	Up
S100a6	Growth arrest and DNA-damage-inducible 45 alpha	0.50	1.21E-03	Up
Ech1	ATP-binding cassette, sub-family C (CFTR/MRP), member 5	0.49	1.68E-03	Up
Olfml3	LKAAEAR motif containing 1 (IKAAEAR murine motif)	-0.22	1.62E-02	Down
Hbb-bs	Calcium channel, voltage-dependent, alpha2/delta subunit 1	-0.22	6.13E-03	Down
Serbp1	Dipeptidylpeptidase 9	-0.22	1.49E-02	Down
Kctd12	Hook microtubule tethering protein 3	-0.22	3.48E-02	Down
Osbp2	THO complex 3	-0.22	3.66E-02	Down
Alox12	Kinesin family member 27	-0.22	1.31E-02	Down
Pigt	Mastermind like 3 (Drosophila)	-0.22	7.06E-03	Down
Scnn1b	Zinc finger protein 638	-0.22	2.81E-02	Down
Epb41l4a	Zinc finger protein 454	-0.22	9.08E-03	Down
Pabpc1	Remodeling and spacing factor 1	-0.22	1.72E-02	Down
Fus	Vomeronasal 1 receptor 19	-0.22	6.55E-03	Down
Rgs5	Lectin, mannose-binding 1 like	-0.22	1.90E-02	Down
Aqp1	Zinc finger, HIT type 6	-0.22	1.99E-02	Down
Ankrd40	Transmembrane and tetratricopeptide repeat containing 4	-0.22	1.78E-02	Down
Casp7	Coagulation factor V	-0.22	1.56E-02	Down
Gstp1	RIKEN cDNA 2310030G06 gene	-0.22	2.12E-02	Down
H2afy	Alpha-kinase 2	-0.22	1.24E-02	Down
Lgmn	Oocyte specific homeobox 6	-0.22	4.10E-02	Down
Plekhs1	FMS-like tyrosine kinase 1	-0.22	2.59E-02	Down
Snap47	Centrosomal protein 63	-0.22	1.23E-02	Down
Pkn1	RIKEN cDNA 1700102P08 gene	-0.22	2.18E-02	Down
Optn	Predicted gene 436	-0.22	3.74E-02	Down
Ide	Isoleucine-tRNA synthetase 2, mitochondrial	-0.22	4.97E-02	Down
Ssbp2	Bridging integrator 3	-0.22	1.27E-02	Down
Ogn	Hyaluronoglucosaminidase 3	-0.22	3.77E-02	Down

DEGs: Differentially expressed genes.

Table 3 The top 25 DEGs of the up-regulated versus down-regulated genes in the GSE26299 dataset (continued)

Name	Description	$\log_2$ fold change	*P*	Up/down
Lcn2	Lipocalin 2	2.87	1.87E-09	Up
Ccl12	Chemokine (C-C motif) ligand 12	2.09	9.22E-09	Up
Steap4	STEAP family member 4	2.07	1.69E-09	Up
Ciapin1	Cytokine induced apoptosis inhibitor 1	2.01	2.37E-06	Up
Defa15	Defensin, alpha, 15	2.00	7.68E-06	Up
Chil1	Chitinase-like 1	1.89	1.48E-12	Up
Sla	Src-like adaptor	1.88	1.58E-06	Up
Csnk2a1	Casein kinase 2, alpha 1 polypeptide	1.81	8.97E-17	Up
Ndel1	nudE neurodevelopment protein 1 like 1	1.81	2.31E-14	Up
Lyz1	Lysozyme 1	1.80	5.07E-10	Up
Edn2	Endothelin 2	1.76	7.52E-12	Up
C3	Complement component 3	1.72	4.79E-07	Up
Neo1	Neogenin	1.67	1.58E-05	Up
AA409587	Casein kinase 2, alpha 1 polypeptide	1.66	5.85E-13	Up
Megf11	Expressed sequence AA409587	1.63	1.45E-13	Up
Slc5a3	Multiple EGF-like-domains 11	1.63	7.70E-11	Up
Gfap	Solute carrier family 5 (inositol transporters), member 3	1.61	3.77E-13	Up
Idh3a	Glial fibrillary acidic protein	1.59	3.61E-10	Up
Pten	Mannosidase 2, alpha 2	1.56	8.18E-15	Up
Riok1	Isocitrate dehydrogenase 3 (NAD+) alpha	1.53	2.28E-06	Up
Npvf	Phosphatase and tensin homolog	1.52	2.57E-11	Up
Tmem56	Cysteine rich protein 61	1.49	1.48E-08	Up
Pla2g6	RIO kinase 1 (yeast)	1.49	2.03E-12	Up
Pot1a	Neuropeptide VF precursor	1.47	1.18E-06	Up
Tagln2	Transmembrane protein 56	1.46	8.08E-12	Up
Tfap2e	UDP-N-acetyl-alpha-D-galactosamine:polypeptide N-acetylgalactosaminyltransferase-like 6	-1.88	2.20E-13	Down
Ddx55	Hyaluronan and proteoglycan link protein 1	-1.85	3.11E-11	Down
Chd3os	Complexin 1	-1.74	7.33E-17	Down
Mro	RIKEN cDNA 1110032F04 gene	-1.67	3.43E-13	Down
Zp3	DiGeorge syndrome critical region gene 8	-1.66	6.61E-15	Down
Atg10	Major urinary protein 10	-1.62	2.81E-02	Down
Myl7	Serine/threonine kinase 32A	-1.61	5.41E-14	Down
Spats1	Leucine-rich repeat LGI family, member 1	-1.56	4.25E-14	Down
Gm9958	T-box 20	-1.56	5.81E-12	Down
Fpr1	Cholinergic receptor, nicotinic, alpha polypeptide 3	-1.56	2.99E-13	Down
Rrm2	Potassium voltage-gated channel, Shal-related family, member 2	-1.55	6.42E-12	Down
Gm2769	Calbindin 2	-1.53	1.52E-17	Down
Rarb	Junction adhesion molecule 2	-1.51	1.95E-14	Down
Mapre3	RIKEN cDNA 4933438K21 gene	-1.50	1.03E-02	Down
Gdf3	RNA binding protein gene with multiple splicing	-1.50	5.59E-10	Down
Nphp3	Neurofilament, heavy polypeptide	-1.48	1.14E-14	Down
Lap3	Adenylate cyclase activating polypeptide 1	-1.42	4.26E-13	Down
Grap	Kit ligand	-1.41	2.16E-14	Down
Saa2	Forkhead box P2	-1.40	2.95E-08	Down
Bpifb3	Copine IV	-1.37	8.54E-13	Down
Ergic3	Anoctamin 3	-1.37	9.29E-12	Down
Mx1	ELAV (embryonic lethal, abnormal vision, Drosophila)-like 2 (Hu antigen B)	-1.35	2.97E-13	Down
Zmym3	cDNA sequence BC048546	-1.31	3.42E-09	Down
Alyref	Regulator of G-protein signaling 4	-1.31	8.02E-12	Down
Rab17	A disintegrin and metallopeptidase domain 10	-1.30	4.21E-10	Down

DEGs: Differentially expressed genes.

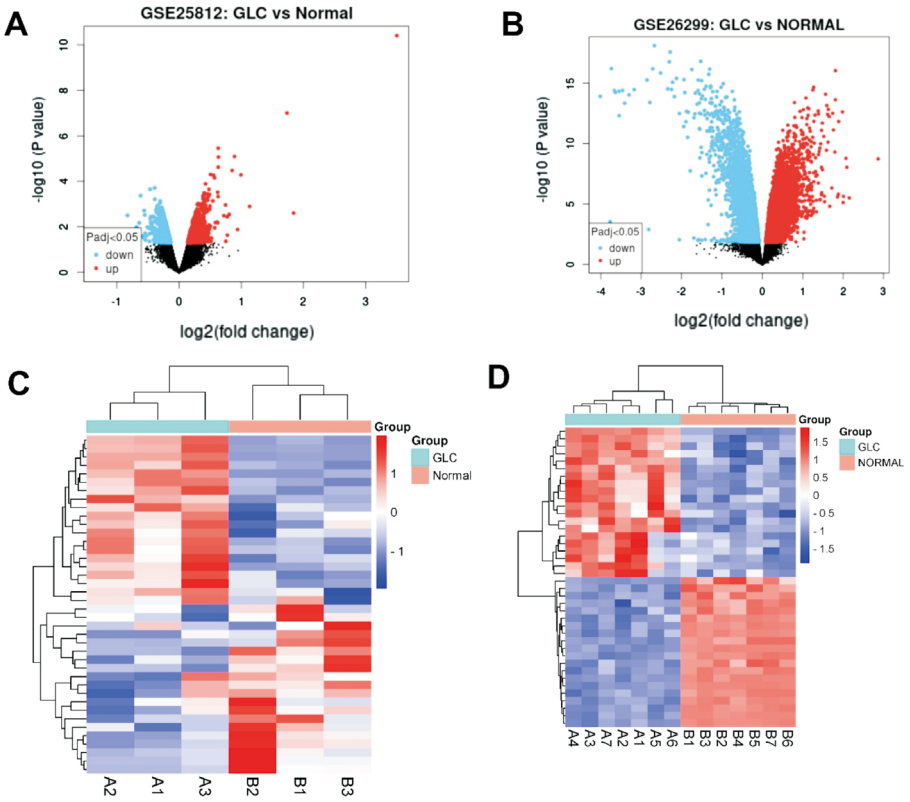

Figure 2 Identification of DEGs for glaucoma A: Volcano plot of DEGs in the GSE25812 dataset. Red dots represent up-regulated genes in the group, and blue dots represent down-regulated genes in the group. B: Volcano plot of DEGs in the GSE26299 dataset. C: Heatmap of the up-regulated versus down-regulated genes ranked the top 25 in the GSE25812 dataset. Red represents highly expressed genes, and blue represents lowly expressed genes. D: Heatmap of the up-regulated versus down-regulated genes ranked the top 25 in the GSE26299 dataset. DEGs: Differentially expressed genes.

Figure 3 Venn diagram for overlapping DEGs in GSE25812 and GSE26299 dataset DEGs: Differentially expressed genes.

identified, including GNAL, BGN, ETS2, FCGP4, MAPK10, MMP15, STAT1, TSPAN8, and VCAM1 (Figure 6).

Biomarkers of Nine Hub Genes for Glaucoma Based on the GSE25812 dataset, the ridge plot of hub genes expression were mapped by the ggridges packages in R software. The results showed that among nine hub genes, the data distribution of MMP15 and STAT1 is relatively dense, and STAT1 had the highest expression. The sample size expressing FCGR4 was the largest (Figure 7). We plotted the ROC curve for nine hub genes by the pROC packages in R software, according to the GSE25812 dataset. The results showed that the AUC values of nine hub genes were greater than 0.8 (Figure 8A-8E), indicating that they could be used as diagnostic biomarkers for glaucoma. Then we performed PCA on nine key genes. Figure 9 showed that a total of two PC axes are generated, including PC1 and PC2. PC1 explained the vast majority of the variance (70.5%), while PC2 provided a lower rate of explanation (11.3%; Figure 9), which illustrating that PC1 could be used to distinguish the glaucoma from the normal eyes.

Construction of a Mouse Model for Glaucoma Next, we constructed a mouse model for glaucoma. HE staining showed that in the control group, ocular tissues such as atrial angle and retina were normal. However, the model group exhibited some ocular hypertension induced retinopathy, such as retinal atrophy and thinning, disorganized cells in the inner and outer nuclear layers, and significantly fewer retinal ganglion cells (Figure 10).

Validation of mRNA Expression of Nine Hub Genes We then performed RT-qPCR to validate the expression of nine genes in glaucoma. The results showed that the mRNA expressions of BGN, ETS2, FCGR4, STAT1, TSPAN8 and VCAM1 were significantly elevated in the model groups compared with the control groups. while the

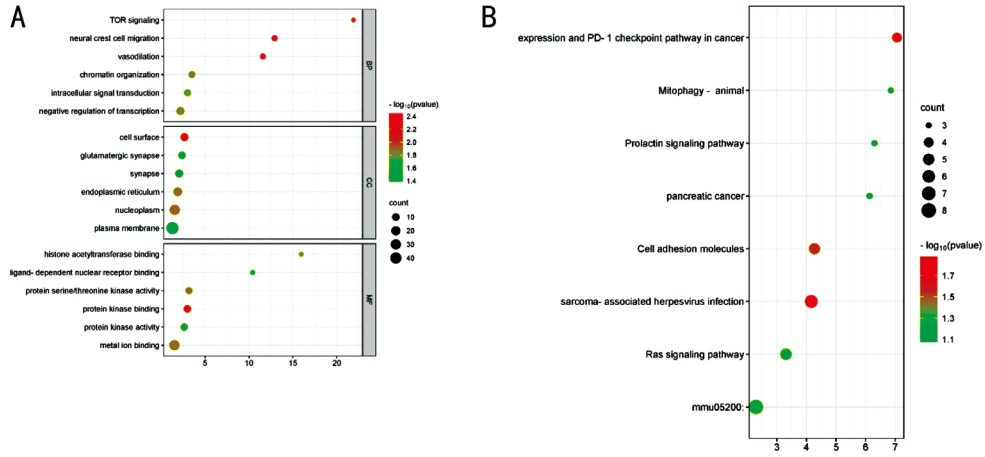

Figure 4 GO annotations and KEGG pathways for overlapping genes A: The top 6 items of the GO annotations are illustrated in a bubble plot. B: The top 8 KEGG pathways are illustrated in a bubble plot. GO: Gene Ontology; KEGG: Kyoto Encyclopedia of Genes and Genomes.

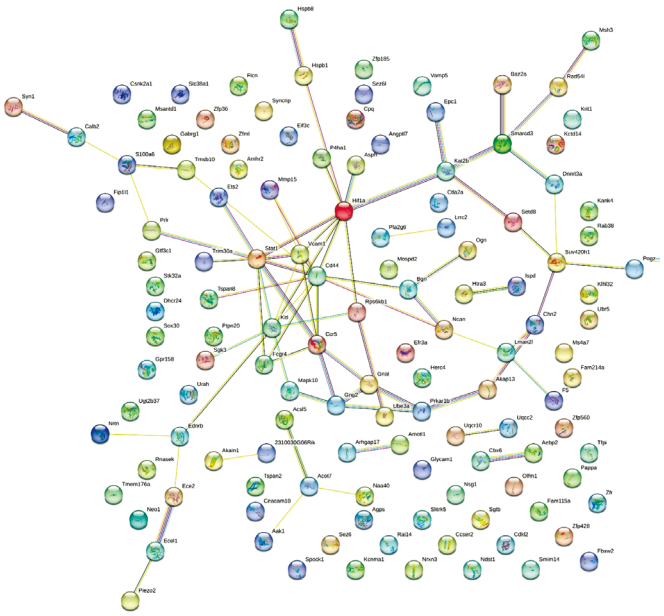

Figure 5 The PPI network of the overlapping DEGs DEGs: Differentially expressed genes; PPI: Protein-protein interactions.

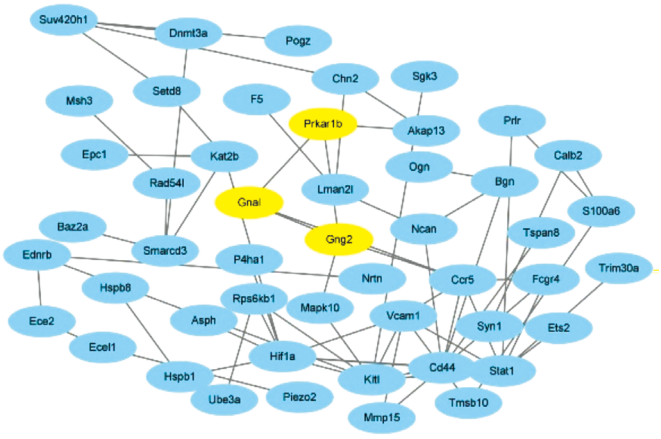

Figure 6 The hub modules of the overlapping DEGs DEGs: Differentially expressed genes.

mRNA expressions of GNAL, MAPK10 and MMP15 were significantly decreased (Figure 11).

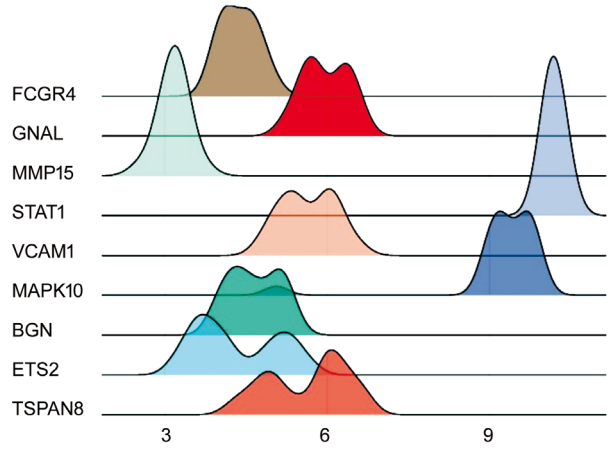

Figure 7 The expression abundance analysis of hub genes The horizontal coordinates represent the amount of gene expression, the shape of the peaks indicates the dispersion between a set of data, and the vertical coordinates represent the number of samples corresponding to the amount of gene expression.

DISCUSSION

The pathophysiology of glaucoma is frequently associated with hereditary factors. Genetic linkage analysis[21], whole exome sequencing[22] and genome-wide association study[23] are used to identify the genes that are responsible for glaucoma[24]. In recent years, an increasing number of genes associated with glaucoma have been revealed. In the trabecular meshwork, the expression of BDKRB1 was significantly reduced after dexamethasone treatment[25]. VEGF plays a crucial and possibly dominant role in the development of intraocular neovascularization and neovascular glaucoma[26]. In the present study, we downloaded the datasets of GSE25812 and GSE26299 from GEO database and finally identified 9 key genes including GNAL, BGN, ETS2, FCGP4, MAPK10, MMP15, STAT1, TSPAN8 and VCAM1. The AUC curve area for the 9 key genes was greater than 0.8, and the PC1 axis composed of them had an interpretation rate of 70.5%

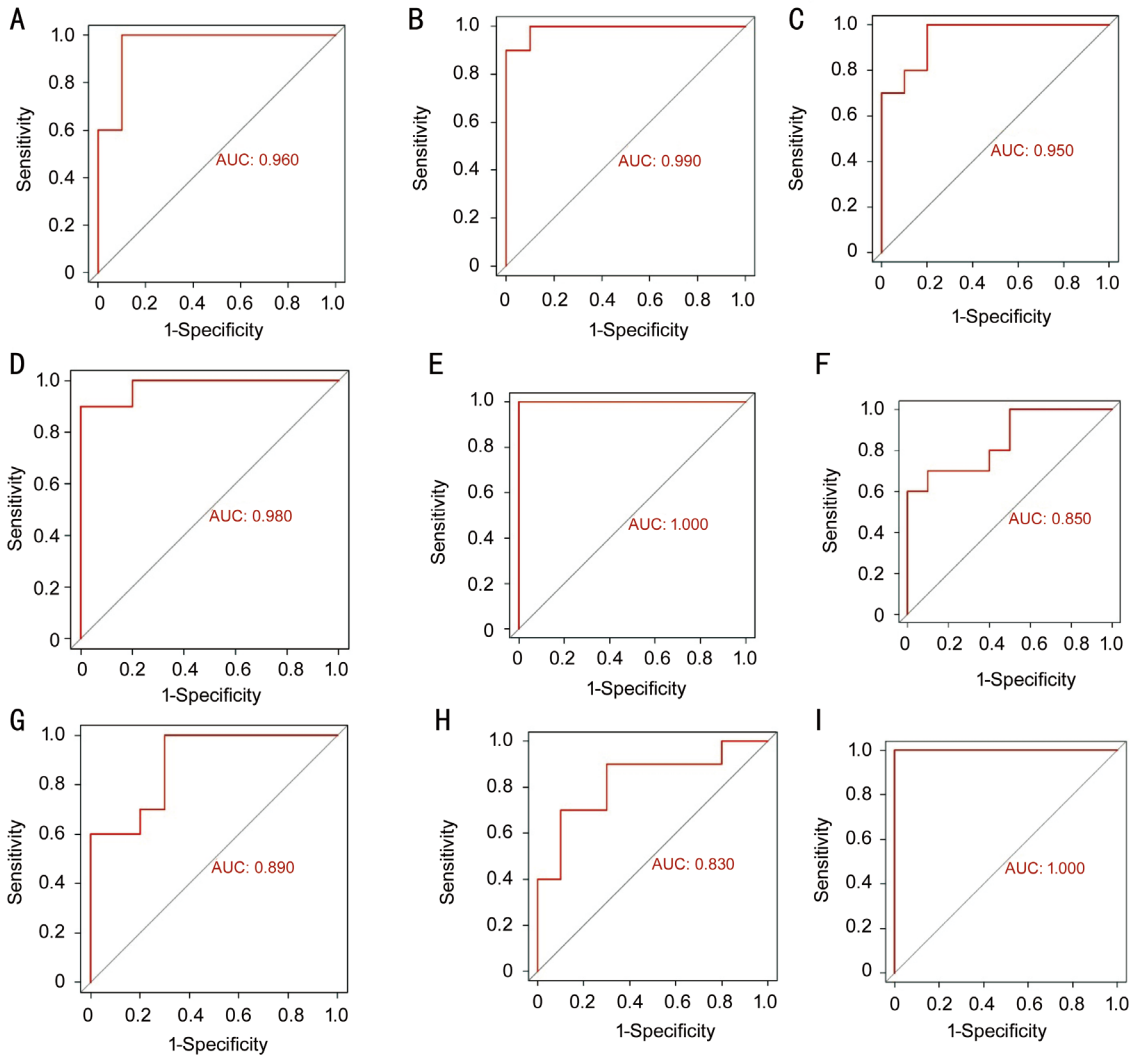

Figure 8 ROC curve analysis of key genes A: GNAL; B: BGN; C: ETS2; D: FCGP4; E: MAPK10; F: MMP15; G: STAT1; H: TSPAN8; I: VCAM1. ROC: Receiver operating characteristic.

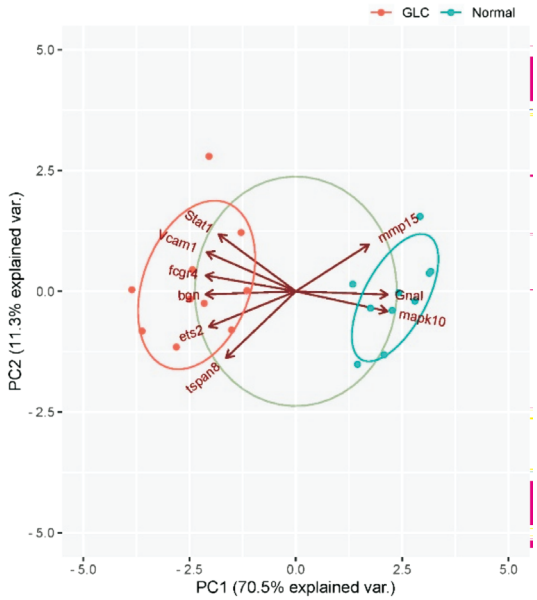

Figure 9 PCA analysis of key genes The coordinate axes PC1 and PC2 of the plot are the first and second principal components (rate of variance explained by latent variables). Dots represent samples and different colors indicate different groupings. PCA: Principal component analysis.

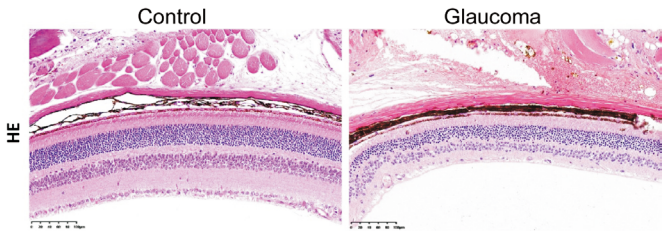

Figure 10 Histological changes in glaucoma was observed by HE staining HE staining: Hematoxylin-eosin staining.

to distinguish glaucoma from normal eyes. Moreover, the expression of BGN, ETS2, FCGR4, STAT1, TSPAN8 and VCAM1 was increased in the mouse model of glaucoma. Conversely, the expression of GNAL, MAPK10 and MMP15 was decreased.

In this study, a total of 128 overlapping DEGs were screened in the GSE25812 and GSE26299 datasets. The utilization of GO and KEGG functional enrichment analyses for DEGs facilitated the identification of genes associated with various biological processes. In the MF category, the DEGs primarily associated with protein kinase binding, protein serine/threonine kinase

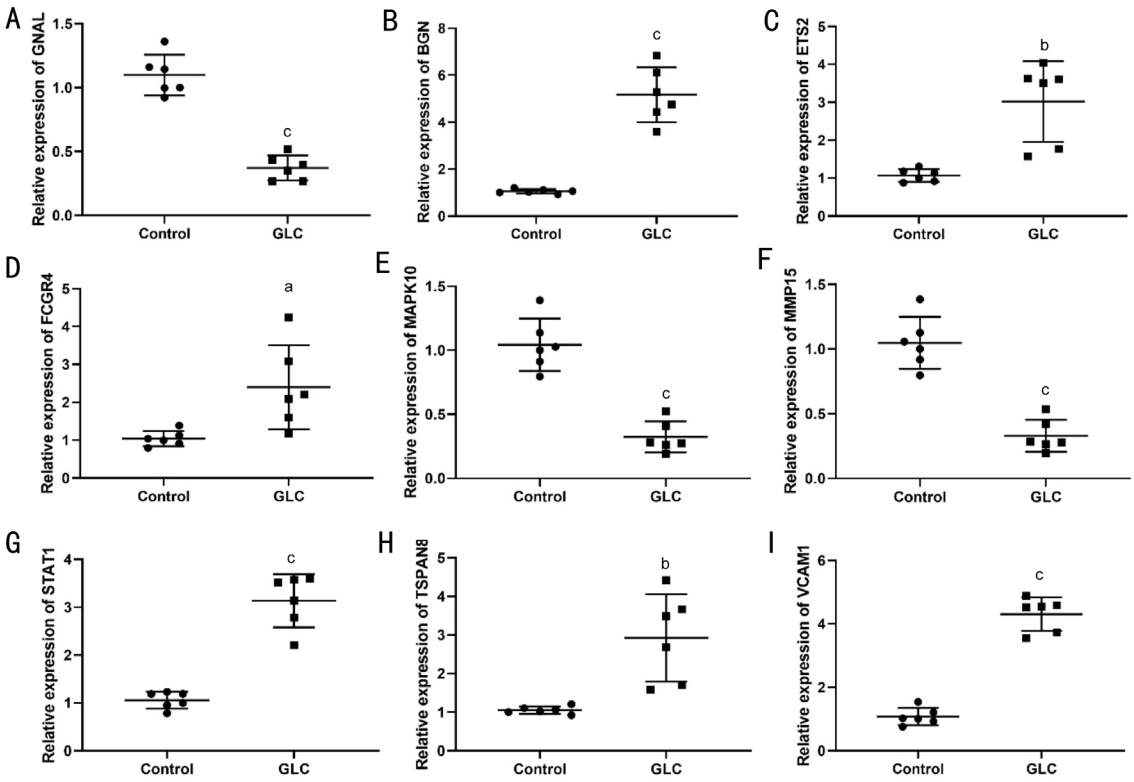

Figure 11 Validation of mRNA expression of 9 hub genes A: RT-qPCR to detect mRNA expression levels of GNAL. B: BGN. C: ETS2. D: FCGR4. E: MAPK10; F: MMP15; G: STAT1; H: TSPAN8; I: VCAM1. [a]*P*<0.05, [b]*P*<0.01, [c]*P*<0.001. RT-qPCR: Real-time reverse transcriptase-polymerase chain reaction; GLC: Glaucoma.

activity and metal ion binding. The previous study has shown that CDC42 binding protein kinase beta is associated with changes in the number of necrotic axons in the optic nerve[27]. Rho kinase, a serine/threonine protein kinase, its inhibitors reduce IOP *in vivo* and *in vitro*[28]. Moreover, a previous study showed that dithiocarbamates ligated with metal ions to exert an anti-glaucoma effect[29]. In the BP category, the DEGs were mainly involved in neural crest cell migration, vasodilation and the target of rapamycin (TOR) signaling, which was consistent with previous findings[30-32]. In the cellular components (CC) category, the DEGs were mainly enriched in the cell surface, nucleoplasm and endoplasmic reticulum, which might be related to the binding of signaling molecules, genetic alterations, and protein metabolic processes[33-34]. In addition, KEGG enrichment analysis showed that the DEGs were mainly enriched in expression and PD-1 checkpoint pathway in cancer, cell adhesion molecules and Ras signaling pathway. Integrins, a group of cell adhesion molecules, are involved in the progression of ocular diseases[35]. The reduction of IOP by Ras inhibitors is most probably by the reestablishment of the extracellular matrix (ECM) homeostasis[36]. In addition, immune response plays an important role in glaucoma, and perhaps immune checkpoint inhibition is a new target for glaucoma treatment[37].

Further studies found that the expression of BGN, ETS2, FCGR4, STAT1, TSPAN8 and VCAM1 was increased in the mouse model of glaucoma. Conversely, the expression of GNAL, MAPK10 and MMP15 was decreased. GNAL, also known as G protein subunit alpha L, encodes a stimulatory G protein alpha subunit. Mutations in GNAL are closely related to dystonia, which are involved in glaucoma[38-40]. VCAM1, a member of the Ig superfamily, produces a cell surface sialoglycoprotein[41]. A genome-wide Meta-analysis identifies VCAM1 as a high-risk gene for primary openangle glaucoma[42]. In the aqueous humor, VCAM1 might be used as a biomarker to predict the progression of diabetic retinopathy, and VCAM1 is overexpressed in the iris of uveitis patients[43-44]. STAT1 encodes a member of the STAT protein family that several ligands, such as interferon-alpha, interferon-gamma, epidermal growth factor, platelet-derived growth factor, and interleukin (IL)-6, can activate. STAT1 is mainly associated with immunity[45-47] and viral infections[48]. In the early period after glaucoma filtration surgery, STAT1 expression was reduced, acting in a manner complementary to STAT3[49]. A study reported that STAT1 expression was upregulated in glaucoma but not significantly changed in optic nerve cross-sections[50]. Differential pathway activity between retinal ganglion cell subpopulations may be regulated by STAT1[51]. ETS2 encodes a transcription factor that regulates development and apoptosis. CDK10 interacts with ETS2 and is involved in corneal epithelial wound healing[52]. Arsenic trioxide inhibits VEGF-A expression in vascular endothelial cells by

upregulating ETS2[53]. In addition, BGN, FCGR4, TSPAN8, MAPK10 and MMP15 were found to be aberrantly expressed in glaucoma for the first time and may be used as biomarkers. Taken together, we hypothesized that the nine hub genes might play an important role in the development of glaucoma.

However, there are several shortcomings in this study. First, through bioinformatics analysis, we found that the DEGs were significantly associated with TOR and Ras signaling pathway, but we only studied the key genes and did not investigate the signaling pathway in depth. Second, functional experiments were not designed due to the limitation of scientific research. Nevertheless, our study still provides new molecular mechanisms and possible therapeutic targets for glaucoma.

In conclusion, a total of 128 DEGs were screened by analyzing the GSE25812 and GSE26299 datasets. These DEGs were associated with protein kinase binding, cell adhesion molecules, and TOR and Ras signaling pathways. Finally, 9 hub genes for glaucoma were screened, including GNAL, BGN, ETS2, FCGP4, MAPK10, MMP15, STAT1, TSPAN8 and VCAM1, which might provide a theoretical basis for clinical application.

ACKNOWLEDGEMENTS

Authors' contributions: Xie RL: conception, design and analysis of data, performed the data analyses and review the manuscript; Nie HY and Xu YX: performed the data analyses and wrote the manuscript. All authors have read and approved the manuscript.

Foundation: Supported by Research Fund of Anhui Institute of Translational Medicine (No.2022zhyx-C73).

Conflicts of Interest: Xie RL, None; **Nie HY,** None; **Xu YX,** None.

REFERENCES

1 Zukerman R, Harris A, Oddone F, Siesky B, Verticchio Vercellin A, Ciulla TA. Glaucoma heritability: molecular mechanisms of disease. *Genes* 2021;12(8):1135.

2 Kang JM, Tanna AP. Glaucoma. *Med Clin North Am* 2021;105(3): 493-510.

3 Saha BC, Kumari R, Sinha BP, Ambasta A, Kumar S. Lasers in glaucoma: an overview. *Int Ophthalmol* 2021;41(3):1111-1128.

4 Lim R. The surgical management of glaucoma: a review. *Clin Exp Ophthalmol* 2022;50(2):213-231.

5 Mehran NA, Sinha S, Razeghinejad R. New glaucoma medications: latanoprostene bunod, netarsudil, and fixed combination netarsudil-latanoprost. *Eye (Lond)* 2020;34(1):72-88.

6 Vallabh NA, Kennedy S, Vinciguerra R, McLean K, Levis H, Borroni D, Romano V, Willoughby CE. Corneal endothelial cell loss in glaucoma and glaucoma surgery and the utility of management with descemet membrane endothelial keratoplasty (DMEK). *J Ophthalmol* 2022;2022:1315299.

7 Xu GH, Chen ZL. Corneal hysteresis as a risk factor for optic nerve head surface depression and retinal nerve fiber layer thinning in glaucoma patients. *Sci Rep* 2021;11(1):11677.

8 Sihota R, Angmo DW, Ramaswamy D, Dada T. Simplifying target intraocular pressure for different stages of primary open-angle glaucoma and primary angle-closure glaucoma. *Indian J Ophthalmol* 2018;66(4):495-505.

9 Allen KF, Gaier ED, Wiggs JL. Genetics of primary inherited disorders of the optic nerve: clinical applications. *Cold Spring Harb Perspect Med* 2015;5(7):a017277.

10 Hauser MA, Sena DF, Flor J, Walter J, Auguste J, Larocque-Abramson K, Graham F, Delbono E, Haines JL, Pericak-Vance MA, Rand Allingham R, Wiggs JL. Distribution of optineurin sequence variations in an ethnically diverse population of low-tension glaucoma patients from the United States. *J Glaucoma* 2006;15(5):358-363.

11 Fingert JH, Robin AL, Scheetz TE, Kwon YH, Liebmann JM, Ritch R, Alward WL. Tank-binding kinase 1 (*TBK1*) gene and open-angle glaucomas (an American ophthalmological society thesis). *Trans Am Ophthalmol Soc* 2016;114:T6.

12 Miller JW. Vascular endothelial growth factor and ocular neovascularization. *Am J Pathol* 1997;151(1):13-23.

13 Chatterjee S, Wang Y, Duncan MK, Naik UP. Junctional adhesion molecule-a regulates vascular endothelial growth factor receptor-2 signaling-dependent mouse corneal wound healing. *PLoS One* 2013;8(5):e63674.

14 Azzolini C, Donati S, Micheloni G, Moretti V, Valli R, Acquati F, Costantino L, Ferrara F, Borroni D, Premi E, Testa F, Simonelli F, Porta G. Expression of *Otx* genes in Müller cells using an *in vitro* experimental model of retinal hypoxia. *J Ophthalmol* 2021;2021:6265553.

15 Azzolini C, Pagani IS, Pirrone C, Borroni D, Donati S, Al Oum M, Pigni D, Chiaravalli AM, Vinciguerra R, Simonelli F, Porta G. Expression of VEGF-A, Otx homeobox and p53 family genes in proliferative vitreoretinopathy. *Mediators Inflamm* 2013;2013:857380.

16 Zhang YJ, Song MM, Bi YW, Lei Y, Sun XH, Chen YH. TIPARP is involved in the regulation of intraocular pressure. *Commun Biol* 2022;5(1):1386.

17 Margeta MA, Yin Z, Madore C, Pitts KM, Letcher SM, Tang J, *et al*. Apolipoprotein E4 impairs the response of neurodegenerative retinal microglia and prevents neuronal loss in glaucoma. *Immunity* 2022;55(9):1627-1644 e7.

18 Gao XR, Huang H, Nannini DR, Fan FD, Kim H. Genome-wide association analyses identify new loci influencing intraocular pressure. *Hum Mol Genet* 2018;27(12):2205-2213.

19 Samsel PA, Kisiswa L, Erichsen JT, Cross SD, Morgan JE. A novel method for the induction of experimental glaucoma using magnetic microspheres. *Invest Ophthalmol Vis Sci* 2011;52(3):1671-1675.

20 Wang JH, Qu DF, An JH, Yuan GM, Liu YF. Integrated microarray analysis provided novel insights to the pathogenesis of glaucoma. *Mol Med Rep* 2017;16(6):8735-8746.

21 Fan BJ, Wang DY, Lam DSC, Pang CP. Gene mapping for primary open angle glaucoma. *Clin Biochem* 2006;39(3):249-258.

22 Rauf B, Khan SY, Jiao XD, Irum B, Ashfaq R, Zehra M, Khan AA, Naeem MA, Shahzad M, Riazuddin S, Hejtmancik JF, Riazuddin SA. Next-generation whole exome sequencing to delineate the genetic basis of primary congenital glaucoma. *Sci Rep* 2022;12(1):17218.

23 Simcoe MJ, Shah A, Fan B, *et al*. Genome-wide association study identifies two common loci associated with pigment dispersion syndrome/pigmentary glaucoma and implicates myopia in its development. *Ophthalmology* 2022;129(6):626-636.

24 O'Connell A, Zhu JL, Stephenson KAJ, Whelan L, Dockery A, Turner J, O'Byrne JJ, Farrar GJ, Keegan D. *MFRP*-associated retinopathy and nanophthalmos in two Irish probands: a case report. *Case Rep Ophthalmol* 2022;13(3):1015-1023.

25 Wei M, Chen LM, Huang ZY, Zhang GW, Guan HJ, Ji M. Expression profile analysis to identify potential gene changes induced by dexamethasone in the trabecular meshwork. *Int J Ophthalmol* 2022;15(8):1240-1248.

26 Călugăru D, Călugăru M. Etiology, pathogenesis, and diagnosis of neovascular glaucoma. *Int J Ophthalmol* 2022;15(6):1005-1010.

27 Stiemke AB, Sah E, Simpson RN, Lu L, Williams RW, Jablonski MM. Systems genetics of optic nerve axon necrosis during glaucoma. *Front Genet* 2020;11:31.

28 Colligris B, Crooke A, Huete F, Pintor J. Potential role of Rho-associated protein kinase inhibitors for glaucoma treatment. *Recent Pat Endocr Metab Immune Drug Discov* 2012;6(2):89-98.

29 Carta F, Aggarwal M, Maresca A, Scozzafava A, McKenna R, Masini E, Supuran CT. Dithiocarbamates strongly inhibit carbonic anhydrases and show antiglaucoma action *in vivo*. *J Med Chem* 2012;55(4):1721-1730.

30 Cibis GW. Congenital glaucoma. *J Am Optom Assoc* 1987;58(9):728-733.

31 Pillunat KR, Pillunat LE. Vasculat treatment concepts in glaucoma patients. *Ophthalmologe* 2021;118(5):431-438.

32 Teotia P, van Hook MJ, Fischer D, Ahmad I. Human retinal ganglion cell axon regeneration by recapitulating developmental mechanisms: effects of recruitment of the mTOR pathway. *Development* 2019;146(13):dev178012.

33 Thomson BR, Liu P, Onay T, Du J, Tompson SW, Misener S, Purohit RR, Young TL, Jin J, Quaggin SE. Cellular crosstalk regulates the aqueous humor outflow pathway and provides new targets for glaucoma therapies. *Nat Commun* 2021;12(1):6072.

34 Anholt RRH, Carbone MA. A molecular mechanism for glaucoma: endoplasmic reticulum stress and the unfolded protein response. *Trends Mol Med* 2013;19(10):586-593.

35 Mrugacz M, Bryl A, Falkowski M, Zorena K. Integrins: an important link between angiogenesis, inflammation and eye diseases. *Cells* 2021;10(7):1703.

36 Agarwal P, Agarwal R. Trabecular meshwork ECM remodeling in glaucoma: could RAS be a target? *Expert Opin Ther Targets* 2018;22(7):629-638.

37 Shestopalov VI, Spurlock M, Gramlich OW, Kuehn MH. Immune responses in the glaucomatous retina: regulation and dynamics. *Cells* 2021;10(8):1973.

38 Erro R, Bhatia KP, Hardy J. GNAL mutations and dystonia. *JAMA Neurol* 2014;71(8):1052-1053.

39 Cuendet JF. Glaucoma and neuro-autonomic dystonia. *Ophthalmologica* 1960;139:286-289.

40 Bessière E, Le Rebeller MS. Glaucoma and neuro-vegetative dystonia. *Bord Med* 1970;3(3):615-623.

41 Pepinsky B, Hession C, Chen LL, *et al*. Structure/function studies on vascular cell adhesion molecule-1. *J Biol Chem* 1992;267(25):17820-17826.

42 Gharahkhani P, Jorgenson E, Hysi P, *et al*. Genome-wide meta-analysis identifies 127 open-angle glaucoma loci with consistent effect across ancestries. *Nat Commun* 2021;12(1):1258.

43 Song S, Yu XB, Zhang P, Dai H. Increased levels of cytokines in the aqueous humor correlate with the severity of diabetic retinopathy. *J Diabetes Complications* 2020;34(9):107641.

44 La Heij E, Kuijpers RW, Baarsma SG, Kijlstra A, van der Weiden M, Mooy CM. Adhesion molecules in iris biopsy specimens from patients with uveitis. *Br J Ophthalmol* 1998;82(4):432-437.

45 Mizoguchi Y, Okada S. Inborn errors of STAT1 immunity. *Curr Opin Immunol* 2021;72:59-64.

46 Zuo YB, Feng Q, Jin LC, Huang F, Miao Y, Liu J, Xu Y, Chen XJ, Zhang HG, Guo TT, Yuan YK, Zhang LT, Wang J, Zheng H. Regulation of the linear ubiquitination of STAT1 controls antiviral interferon signaling. *Nat Commun* 2020;11(1):1146.

47 Kang YH, Biswas A, Field M, Snapper SB. STAT1 signaling shields T cells from NK cell-mediated cytotoxicity. *Nat Commun* 2019;10(1):912.

48 Tolomeo M, Cavalli A, Cascio A. STAT1 and its crucial role in the control of viral infections. *Int J Mol Sci* 2022;23(8):4095.

49 Watanabe-Kitamura F, Ogawa A, Fujimoto T, Iraha S, Inoue-Mochita M, Watanabe T, Takahashi E, Tanihara H, Inoue T. Potential roles of the IL-6 family in conjunctival fibrosis. *Exp Eye Res* 2021;210:108708.

50 Yang ZY, Quigley HA, Pease ME, Yang YQ, Qian J, Valenta D, Zack DJ. Changes in gene expression in experimental glaucoma and optic nerve transection: the equilibrium between protective and detrimental mechanisms. *Invest Ophthalmol Vis Sci* 2007;48(12):5539-5548.

51 Ivanov D, Dvoriantchikova G, Barakat DJ, Nathanson L, Shestopalov VI. Differential gene expression profiling of large and small retinal ganglion cells. *J Neurosci Methods* 2008;174(1):10-17.

52 Zehra M, Mushtaq S, Ghulam Musharraf S, Ghani R, Ahmed N. Author correction: association of cyclin dependent kinase 10 and transcription factor 2 during human corneal epithelial wound healing *in vitro* model. *Sci Rep* 2020;10(1):14405.

53 Ge HY, Han ZJ, Tian P, Sun WJ, Xue DX, Bi Y, Yang ZH, Liu P. VEGFA expression is inhibited by arsenic trioxide in HUVECs through the upregulation of ets-2 and miRNA-126. *PLoS One* 2015;10(8):e0135795.